SSRG International Journal of Recent Engineering Science
ISSN: 2349–7157 / https://doi.org/10.14445/23497157/IJRES-V11I6P118

Volume 11 Issue 6, 216-224, Nov-Dec 2024

Original Article

Design of a Pump in an Organic Rankine Cycle Using R-600a as the Working Fluid for a 150 kW Capacity System

Sri Wuryanti[1*], Muhammad Rizki[1]

[1]*Department of Energy Conversion Engineering, Politeknik Negeri Bandung, Bandung 40559, Indonesia.*

[1]*Corresponding author : sriwuryanti.lamda@gmail.com*

Received: 22 October 2024 Revised: 26 November 2024 Accepted: 15 December 2024 Published: 29 December 2024

Abstract *- The pump is one of the main components of the Organic Rankine Cycle (ORC), responsible for circulating the working fluid, which in this design is refrigerant-600a. The mathematical design of this pump begins by inputting initial data on the brine used as the heating fluid in the ORC. This data was obtained by simulating a pump in a Rankine cycle system, resulting in a temperature of 176°C, a pressure of 9.65 bar, and a flow rate of 159,210.92 kg/h. The main design requirement is that the total head and NPSH (Net Positive Suction Head) required must not exceed the NPSH available. The magnitudes of these parameters are 6.00 m and 2.71 m, respectively. Next, the core components of the pump, namely the impeller, casing, and shaft, are designed, and the materials chosen for these components are adjusted according to standardization requirements. Based on the mathematical design results, it was found that the pump operates at a pressure of 6.8 bar on the suction side and 9.5 bar on the discharge side with a capacity of 2.68 kg/s, a pump head of 54 m, and a total of 6 blades. The pump is designed to operate at 1500 rpm with a power of 17.30 kW and a pump efficiency of 80%.*

Keywords *- Centrifugal pump, Fluid, Organic Rankine cycle, Refrigerant-600a.*

1. Introduction

Pumps are widely used in both industry and households. Industrial applications include cooling towers, boilers, and reactor cooling systems. Pumps are crucial equipment in water treatment plants as they move water from one part of the installation to another. Pumps operate under two-phase flow conditions in the petroleum industry, chemical processing, water conservancy, irrigation, and other fields [1, 2]. The arrangement of the blades on the pump affects the physics of the flow and dynamic performance. Numerical simulation is a verification approach to investigate these aspects. Volute design accommodates radial impellers with the same outlet diameter [3]. Energy can be saved by adjusting pump flow rates closer to load requirements or eliminating excessive pressure drops. Decisions made during the design process can significantly affect the operation of pumps [4, 5]. Expanding the efficient operating zone and increasing the energy efficiency of optimized centrifugal pumps can be achieved by improving the fit between the rotor and the stator [6]. In households, the water flow system from the storage tank to the bathroom and washing tub aims for space-saving, and a new sink-style dishwasher features an innovative pump [7]. Research on magnetic vortex pumps' external and internal flow characteristics shows that the pump head rises by 16.7% with increasing medium temperature [8]. According to theoretical studies, working fluids such as R123, R134a, R600, and R290 operate at temperatures below 120°C, offering high thermal efficiency and environmental friendliness [9]. An analysis of the ORC system using environmentally friendly working fluids shows that the evaporator and condenser temperatures significantly influence the ORC's energetic performance [10]. This study aims to use R-600a because it offers better thermodynamic efficiency compared to R134a, providing more efficient cooling performance with lower energy consumption and a low Global Warming Potential (GWP) of around 3. R-600a is considered safer because it is non-toxic and non-flammable under the right conditions. However, as a hydrocarbon, R-600a is highly flammable, so equipment using this refrigerant must be equipped with proper fire protection. This study's novelty lies in using R-600a in the ORC cycle, which results in a pump efficiency of 80%.

1.1. Centrifugal Pump on the Rankine Cycle

Centrifugal pumps consist of an impeller located in the center of an inlet channel. When the impeller rotates, fluid flows into the casing surrounding the impeller due to centrifugal force. This casing reduces the fluid speed while maintaining the high rotational speed of the impeller. The casing converts the fluid velocity into pressure, allowing the fluid to exit through the outlet. The advantages of this type of pump include low cost, smooth flow, high-speed operation, and uniform pressure.

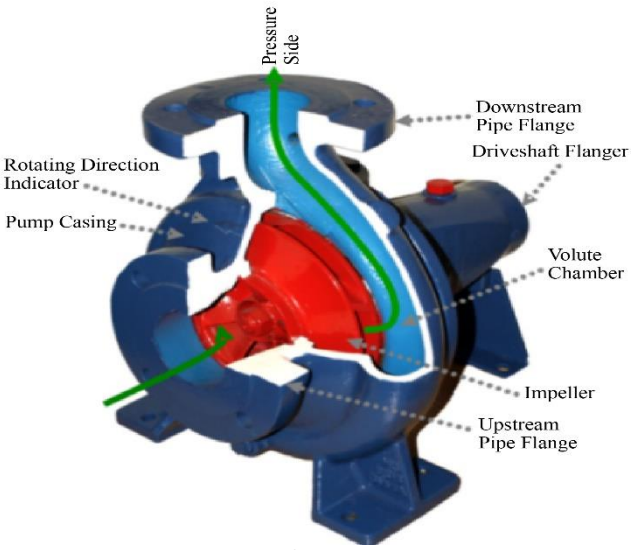

Fig. 1 Centrifugal pump [11]

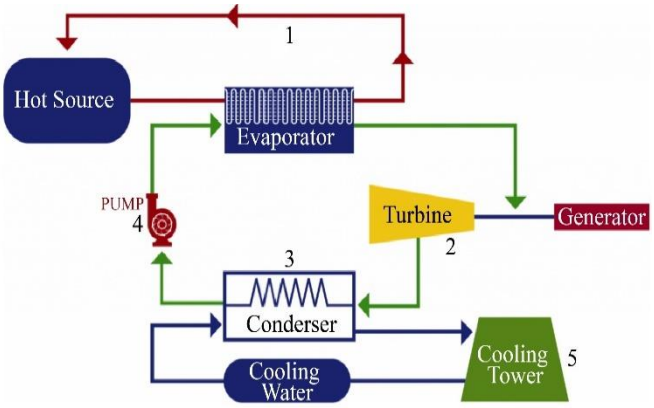

Fig. 2 Organic Rankine Cycle [12]

The pump in this cycle plays a vital role in maintaining the continuity of the electricity generation process. It channels fluid from the condenser (condensation result) to the re-cooperator for reheating and then to the evaporator, where it is heated and changes its phase to steam. The Organic Rankine Cycle (ORC) designed in this paper for the Geothermal Power Plant serves as a reference for obtaining conditions from the brine data used in the cycle.

The brine has a temperature of approximately 127°C, derived from the separation of steam from water in the separator component of the geothermal power plant. The working fluid used in this cycle is refrigerant type R-600a, chosen because its boiling point is much lower than water.

This R-600a refrigerant has a Global Warming Potential (GWP) value, a relative measure of the heat trapped by greenhouse gases. Additionally, it has an Ozone Depletion Potential (ODP) value, a relative measure of the degradation of the ozone layer caused by a compound. Lower GWP and ODP values indicate that the fluid is environmentally friendly [13].

1.2. Organic Rankine Cycle (ORC) Simulation

The initial simulation of this ORC cycle has a capacity of 150 kW. The input data used is brine data from the geothermal power plant (PLTP) with a pressure of 9.65 bar, a temperature of 176°C, and a flow rate of 159,210.92 kg/h.

The initial parameters needed for pump design in the ORC cycle are the temperature, pressure, and mass flow rate on both the input and output sides [14, 15]. A schematic of the ORC cycle from the simulation results is shown in Figure 3.

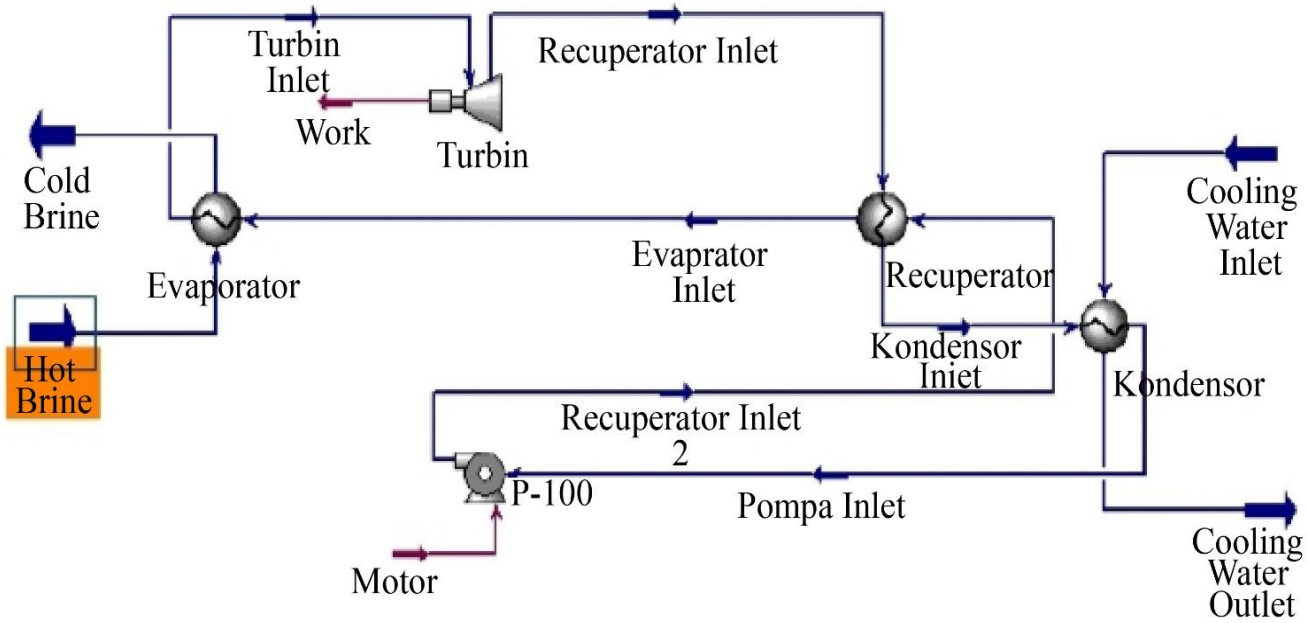

Fig. 3 ORC cycle simulation results

Table 1. Initial parameters of simulation results

Parameter	Suction		Discharge	
	Value	Unit	Value	Unit
Pressure (P)	6.8	Bar	9.5	Bar
	680000	Pa	950000	Pa
Mass flow rate (ṁ)	26.8	kg/s	26.8	kg/s
Volume flow rate (Q)	0.0475	m^3/s	0.0475	m^3/s
	171	m^3/h	171	m^3/h
Temperature (T)	34	℃	34	℃
Density (ρ)	544.3	kg/m^3	544.3	kg/m^3
Kinematic viscosity (v)	2.862×10^{-7}	m^2/s	2.862×10^{-7}	m^2/s
Pipe inner diameter (D)	0.1625	m	0.1524	m

2. Methods

2.1. Mathematical Design Stages

The parameters in Table 1 are used to design a pump for the ORC installation (Figure 2), where the pump circulates working fluid from the condenser, which is situated 2 meters in height and 3 meters away from the input side of the pump, to the evaporator, which is 4 meters away and 5 meters in height. The installation includes 4 gate valves: 1 on the suction and 3 on the output sides. The prime mover designed the pump as a synchronous motor with a capacity of 17.89 kW, 4 poles, and an operating frequency of 50 Hz. This pump will rotate at a constant speed of 1500 rpm.

2.1.1. Pump design considerations include

- Ensuring the pump does not experience cavitation by maintaining NPSH available (NPSH av) greater than NPSH required (NPSH req) [16].
- $\frac{f_s \times Sf_2}{\alpha \, atau \, \beta} \geq f_g \times K_t \times C_b$

The mathematical approach to pump design in Organic Rankine Cycle (ORC) installations involves analyzing the thermodynamics of the cycle and applying the laws of physics related to energy transfer and fluid flow. The pump in an ORC installation plays a primary role in pumping the working fluid from the condenser to the evaporator, increasing the pressure of the fluid so that it can absorb heat energy during the heating process.

2.1.2. The assumptions used include

Adiabatic Process

The pump process is considered adiabatic, meaning there is no heat exchange with the environment during pumping.

Steady-State Flow

The fluid flow entering and leaving the pump is considered in a steady-state condition, meaning the mass flow rate does not change over time.

Neglect of Energy Losses

Energy losses in the pump system, such as friction or heat loss to the environment, are typically considered small or neglected in basic calculations.

Ideal Working Fluid Properties

The working fluid properties are treated as ideal fluids.

Isentropic Conditions

Some ideal pump designs assume that the pumping. process is isentropic.

2.1.3. Provisions are as follows

Shear Stress According to ASME Standards

The safety factor (Sf_1) is taken as 5.6 for the SF material type (with guaranteed strength) and 6.0 for the S-C material type (considering the influence of mass and alloy steel). Sf_2 is used to review the cross-section of the shaft, which will have a key-way or stepped shape. The Sf_2 value for alloy steel ranges between 1.3 and 3.0.

Shaft Diameter Planning

The correction factor is taken according to the type of shaft loading. The twisting moment correction factor (Kt) for rotational loading is 1.5. The bending load correction factor (Cb) is 1.0 when there is no significant bending load on average (see Table 2).

2.2. Pump Design Results

The pump design, which uses environmentally friendly R-600a fluid and considers the installation details, including the pump location, piping, valves, and pressure tank, achieved an efficiency of 80%.

The pump design results, including pump specifications and dimensions, are shown in Tables 4 and 5. The shaft, blade, and pin drawings are depicted in Figure 5.

Table 2. Load type correction factor

No	Loading Type	C_b	K_t
1	Fixed Shaft		
	a. Load Slowly	1	1
	b. Sudden burden	1.5 - 2	1.5 - 2
2	Rotating shaft		
	a. Smooth impact load	1.2	1
	b. Light impact/shock loads	1.2 - 1.75	1 - 1.5
	c. Impact load / Heavy shock	1.75 - 2.3	1.5 - 3

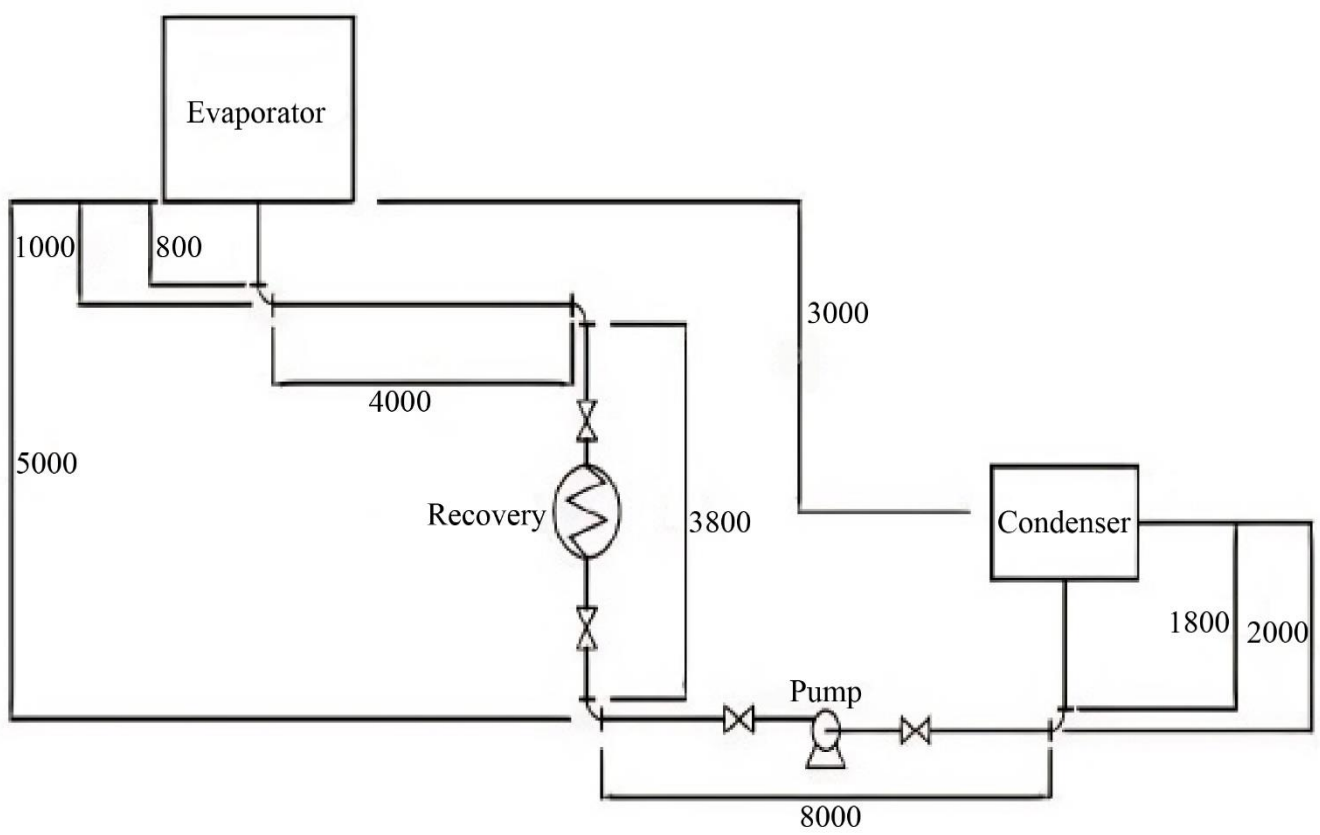

Fig. 4 Pump installation on ORC

Table 3. Mathematical design stages

No	Equation	Results	Unit
1	Qp = Pump capacity + (10% pump capacity)	25.91	kg/s
2	Qtp = $\frac{Qp}{\rho}$ (ρ R-600a = 544.3 kg/m^3)	0.0476	m^3/s
3	$H_s = \left(\left(\frac{P_2}{\rho g} + \frac{C_2^2}{2g} + z_2\right) - \left(\frac{P_1}{\rho g} + \frac{C_1^2}{2g} + z_1\right)\right)$	54.86	m
4	$C = \frac{Q}{A}$	2.29	m/s
5	$C = \frac{Q}{\frac{\pi}{4} x D^2}$	2.61	m/s
6	$h_l = f\frac{L}{D}\frac{C^2}{2g}$	0.4769	m
7	$Re = \frac{CD}{v}$(input)	1,331,339	
8	$h_{lm} = K\frac{C^2}{2g}$	0.607	m
9	$H = \left(\left(\frac{P_2}{\rho g} + \frac{C_2^2}{2g} + z_2\right) - \left(\frac{P_1}{\rho g} + \frac{C_1^2}{2g} + z_1\right)\right) + (h_l + h_{lm})$	55.45	m
10	$Re = \frac{CD}{v}$(output)	1,416,865.1	
11	Nm= $\frac{120\,F}{p} \times (1-s)$	1500	rpm
12	$n_s = 3{,}65\,\frac{n\sqrt{Q}}{H^{3/4}}$	58.78	rpm

13	$n_{sq} = \frac{n\sqrt{Q}}{H^{3/4}}$	124.74	rpm
14	$NPSH_{av} = \frac{P_1}{\rho} - \frac{P_v}{\rho} \pm z_1 - h_{ls}$	5.96	m
15	$\sigma = \frac{(ns)^{4/3}}{S}$	0.048	m
16	$NPSH_{req} = H_{sv} = \sigma$ x H	2.71	m
17	$D_1 = (4{,}5 - 4{,}0)\ x\ 10^3 x \sqrt[3]{\frac{Q}{n}}$	126.64	mm
18	$\eta_h = 1 - \frac{0{,}42}{(log\ D_1 - 0{,}172)^2}$	88	%
19	$\eta_v = \frac{1}{1 + (0{,}68\ x\ n_s^{-2/3})}$	95	%
20	$\eta = \eta_h\ x\ \eta_v\ x\ \eta_m$ (η mekanik 95%)	80	%
21	$N_o = \frac{g\ x\ \rho\ x\ Q\ x\ H}{1000}$	14.09	kW
22	$N_i = \frac{N_o}{\eta}$	17.6	kW
23	$N_i = (100\% + \%\ daya\ cadangan)\ \times\ N_i$	20. 24	
24	$T = \frac{N_i}{\omega}$	0.125	k N/m
25	$f_s = \frac{f_m}{S_{f1} \times S_{f2}}$	51,667	k N/m^2
26	$d_s = \sqrt[3]{\frac{16\ \times\ T\ \times\ K_t\ \times\ C_b}{\pi\ \times\ f_s}}$	24.663	mm
27	$\frac{f_s\ \times\ Sf_2}{\alpha\ atau\ \beta} \geq f_g\ \times\ K_t\ \times\ C_b$	93,939.39≥ 28,707.6	k N/m^2
28	$f_g = \frac{16\ \times\ T}{\pi\ \times\ {d_s}^3}$	23,923.17	k N/m^2
29	$d_h = (1{,}2 - 1{,}3)\ \times\ d_s$	39	mm
30	$Q_{th} = \frac{Q}{\eta_v}$	0.0497	m^2/s
31	$C_0 = \frac{4\ x\ Q_{th}}{\pi\ x\ {D_s}^2}$	3	m/s
32	$C_{m0} = (1.05 - 1.1)\ C_0$	3.04	m/s
33	$B_1 = \frac{Q_{th}}{\pi\ \times\ D_1\ \times\ C_{m0}}$	41.2	mm
34	$C_{m1} = K_1 \times\ C_{m0}$	3.643	m/s
35	$u_1 = \frac{\pi\ x\ D_1\ x\ n}{60}$	9.94	m/s
36	$\beta_{10} = tan^{-1}\left(\frac{C_{m1}}{u_1}\right)$	20.12	o
37	$\beta_1 = \beta_{10} + \delta$	25.12	o
38	$H_{th} = \frac{H}{\eta_h}$	62.49	m
39	$u_2 = \sqrt{\frac{g\ \times\ H_m}{\bar{C}u2}}$	27.68	m/s
40	$C_{m3} = 0.8\ \times\ C_{m0}$	2.42	m/s

41	$D_2 = \frac{60 \times u_2}{\pi \times n}$	0.35	m
42	$\beta_2 = sin^{-1}\left(\sin\beta_1 \times \frac{K_2}{K_1} \times \frac{w_1}{w_2} \times \frac{C_{m3}}{C_{m0}}\right)$	23.42	o
43	$C_{m2} = (0.85 - 0.9) \times C_{m1}$	3.09	m/s
44	$Z = 6{,}5 \times \frac{D_2 + D_1}{D_2 - D_1} \times \sin\left(\frac{\beta_1 + \beta_2}{2}\right)$	6	
45	$H_{th\infty} = (1 + p)\, H_m$	80.88	m
46	$\psi = (0{,}55 - 0{,}68) + 0{,}6 \sin\beta_2$	0.76	
47	$p = \frac{2\Psi}{Z} \times \frac{1}{1 - \left(\frac{D_1}{D_2}\right)^2}$	0.29	
48	$u_2 = \frac{C_{m2}}{2 \times \tan\beta_2} + \sqrt{\left(\frac{C_{m2}}{2 \times \tan\beta_2}\right)^2 + (g \times H_\infty)}$	31.29	m/s
49	$D_2 = \frac{60 \times u_2}{\pi \times n}$	0.407	m
50	$C_{m3} = \frac{C_{m2}}{K_2}$	2.81	m/s
51	$B_2 = \frac{Q_{th}}{\pi \times D_2 \times C_{m3}}$	18.49	mm
52	$K_1 = \frac{1}{1 - \frac{Z \times \delta_1}{\pi \times D_1 \times \sin\beta_1}}$	1.14	
53	$K_2 = \frac{1}{1 - \frac{Z \times \delta_2}{\pi \times D_2 \times \sin\beta_2}}$	1.05	
54	$w_1 = \frac{C_{m1}}{\sin\beta_1}$	8.58	m/s
55	$w_2 = \frac{C_{m2}}{\sin\beta_2}$	7.78	m/s

Table 4. Pump specifications

Parameter	Value	Unit
Pump Type	Centrifugal	
Capacity	25.91	kg/s
Number of Levels	1	
Head Total	54	m
$NPSH_{req}$	2.71	m
$NPSH_{av}$	5.96	m
Round	1500	rpm
Pump Power	17.89	kW
Efficiency	80	%

Table 5. ORC Pump Dimensions

Parameter	Value	Unit
Shaft diameter	24.663	mm
Inlet diameter	126.64	mm
Inlet angle	28	
Width of entry side	41.2	mm
Side exit diameter	352	mm
Outward blade angle	23	
Exit side width	18.49	mm
Number of blades	6	

3. Discussion

Net Positive Suction Head (NPSH) is a critical factor in pump design that ensures the pump operates without cavitation, which can cause damage to the pump and reduce its performance. The NPSH calculation is fundamental to the design and operational conditions of pumps, particularly in systems such as the Organic Rankine Cycle (ORC), where working fluids are circulated under varying temperature and pressure conditions. The design results demonstrate that NPSH av is greater than NPSH req, leading to an efficiency of 80%. This efficiency significantly improved over previous research, which reported a pump efficiency of 63%[17]. This efficiency improvement can be attributed to several factors, including optimization of NPSH conditions and better pump design choices (e.g., impeller design, operating conditions, etc.).

A minimum flow rate of 100 L/s (0.1 m³/s) was established, which ensures the pump operates within the ideal efficiency range. The performance prediction suggests that the pump will maintain an efficiency better than 80%[18] at this flow rate, which is critical in ensuring the system's overall performance. The model presented in this paper successfully meets the design criteria, particularly ensuring that NPSH av is greater than NPSH req. This guarantees that the pump operates free from cavitation, improving its reliability and efficiency. Furthermore, the efficiency achieved at 80% represents a significant improvement over previous research, highlighting the effectiveness of the design. The comprehensive analysis of Euler's head, theoretical head, actual head, and capacity under varying rotational speeds provides additional insight into the pump's performance, ensuring the system can operate efficiently across various conditions.

3.1. Head Euler

The Euler head is assumed to be ideal because friction flow is considered zero, free from pipe turbulence, and has infinite blades. The equation below is used to calculate the value of the Euler head.

$$(H_{th}\infty) = 103{,}87 - 339{,}75\ Q_v \qquad (1)$$

3.2. Theoretical Head

The theoretical head is the opposite of the Euler head, where this head considers losses and the number of blades. The equation below is a way to get the value of the theoretical head.

$$H_{th} = \frac{H_{th\infty}}{1+c_p} \qquad (2)$$

Inserting equation (2) into equation 3 and Cp (Pfleiderer coefficient chosen 0.4), then the equation becomes:

$$H_{th} = 74{,}19 - 242{,}67\ Q_v \qquad (3)$$

3.3. Actual Head

The actual head is the head value in the pumping process that occurs in actual conditions. The value of the actual head can be smaller when compared to the theoretical head; this happens because of losses in the flow, namely shock loss and friction loss. Below is the equation to get the value of the actual head.

$$H_{actual} = H_{th} - h_h \qquad (4)$$

$$h_h = h_{fd} + h_s \qquad (5)$$

$$h_{fd} = (1 - \eta_h)\ H_{th}\ \left(\frac{Q_v}{Q}\right)^2 \qquad (6)$$

$$h_s = \frac{k_{sh}}{2g}\left(u_1{}^2 + \left(u_2\left(\frac{1}{1+c_p}\right)\frac{D_2}{D_3}\right)^2\right)\left(1 - \frac{Qv}{Q}\right)^2 \qquad (7)$$

Inserting equations (3), (5), (6), and (7) into equation (4) and the parameters obtained from the design (Table 3), the equation becomes:

$$H_{actual} = 75{,}87 + 857{,}73\ Q_v - 15.958{,}97\ Q_v{}^2 \qquad (8)$$

From the design results, a discharge of 0.0476 m³/s was obtained. By varying the discharge value from 10% to 90%, a comparison of the Euler head, theoretical head, and actual head values was achieved. The analysis calculates the Euler head, theoretical head, and actual head of the pump according to equations (1, 3, and 8), determining the heat generated by the pump based on the discharge value. The pump curve shows measurable relationships between these variables. The results of the head calculations are depicted as a head dependence curve on the volume flow rate in Figure 5. Figure 5 shows the relationship between head and volume flow rate. The head decreases linearly until it reaches a minimum value for the Euler and theoretical heads, while the actual head increases and then decreases. Under operating conditions, pump performance is much more difficult to predict, so various definitions of pressure loss must be considered. Increased hydraulic losses and losses in the impeller and intermediate disk diffuser are the dominant factors [19].

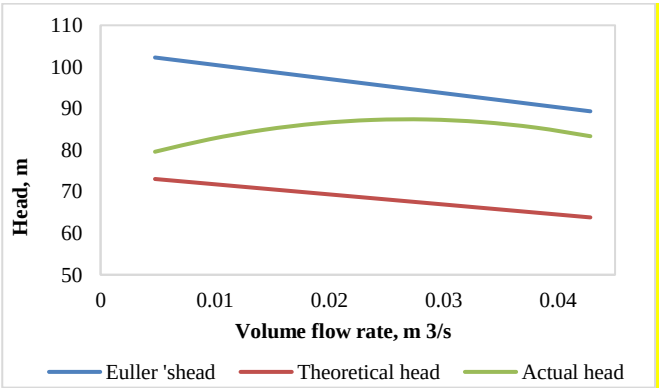

Fig. 5 Pump characteristic curve

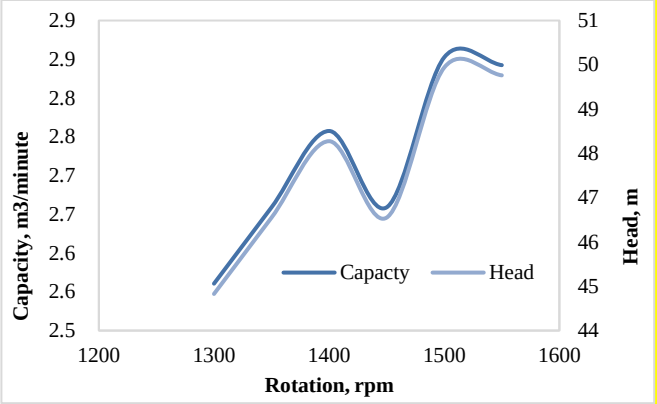

Fig. 6 Rotation versus head and capacity

The pump characteristics from the relationship of head-to-volume flow rate are decreasing, which is consistent with the characteristics of centrifugal pumps [20, 21].

3.4. Capacity and Head Values Due to Changes in Rotation

This calculation varies the rotation of the pump drive by differences of 50 rpm around the nominal 1450 rpm used in this design, with variations at 1350 rpm, 1400 rpm, 1450 rpm, 1500 rpm, and 1550 rpm. The equation below calculates the capacity due to changes in rotation.

$$\frac{Q_n}{Q_v} = \frac{n_n d_n^3}{n_v d_v^3} \tag{9}$$

By inserting the parameters from Table 3 into equation (9), the equation becomes:

$$Q_v = Q_n \frac{n_v}{1450} \tag{10}$$

The equation below is a way to calculate the capacity due to changes in rotation.

$$\frac{H_n}{H_v} = \frac{n_n d_n^3}{n_v d_v^3} \tag{11}$$

By inserting the parameters from Table 3 into equation (11), the equation becomes:

$$H_v = H_n \frac{n_v}{1450} \tag{12}$$

The relationship between capacity and head with rotation variations is depicted in Figure 6. Such curves help understand and predict the pump's performance under different operating conditions. Figure 6 shows the highest pump capacity at 1500 rpm, 2.85 m³/s, and the highest head at 1500 rpm, 49.94 m. At low rotation speeds, the head increases as speed increases because the pump imparts more energy to the fluid. However, the head might peak and decrease as rotation speed increases due to cavitation or other inefficiencies. After surpassing the inefficiency zone, with a further increase in rotation speed, the head might increase again if the pump design allows for better efficiency at higher speeds. The flow rate increases with speed at low rotation speeds because the pump moves more fluid with each rotation. At certain speeds, the flow rate is reduced due to cavitation, where vapor bubbles form and collapse, reducing performance. Beyond this point, as the rotation speed continues to increase, the flow rate can increase again if the pump overcomes the effects of cavitation or is designed to operate efficiently at a higher speed.

4. Conclusion

The pump is designed for the Organic Rankine Cycle with a capacity of 150 kW to distribute type R-600a refrigerant fluid from the condenser to the evaporator through the recuperator, successfully distributing 0.0476 m³/s or 2.82 m³/minute. The simulation results show that the input pressure (suction) is 6.8 bar, the output pressure (discharge) is 9.5 bar, and the temperature is 34.45°C.

Acknowledgements

The authors acknowledge this and thank UPPM Politeknik Negeri Bandung, who supports the research funding. The Department of Energy Conversion Engineering Politeknik Negeri Bandung provides the laboratory facility for the research.

Contributions

SW conceived and designed the research—SW and MR wrote and analyze the data.

References

[1] Qifeng Jiang et al., "A Review of Design Considerations of Centrifugal Pump Capability for Handling Inlet Gas-Liquid Two-Phase Flows," *Energies*, vol. 12, no. 6, pp. 1-18, 2019. [CrossRef] [Google Scholar] [Publisher Link]

[2] Yue Zhang, and Chenchen Song, "A Novel Design of Centrifugal Pump Impeller for Hydropower Station Management Based on Multi-Objective Inverse Optimization," *Processes*, vol. 11, no. 12, pp. 1-20, 2023. [CrossRef] [Google Scholar] [Publisher Link]

[3] Biaobiao Wang et al., "Effect of Short Blade Circumferential Position Arrangement on Gas-Liquid Two-Phase Flow Performance of Centrifugal Pump," *Processes*, vol. 8, no. 1317, pp. 1-14, 2020. [CrossRef] [Google Scholar] [Publisher Link]

[4] Konrad Bamberger et al., "Development, Validation, and Application of an Optimization Scheme for Impellers of Centrifugal Fans Using Computational Fluid Dynamics-Trained Metamodels," *Journal of Turbomachinery Transactions of the Asme*, vol. 142, no. 11, pp. 1-7, 2020. [CrossRef] [Google Scholar] [Publisher Link]

[5] Ehsan Abdolahnejad, Mahdi Moghimi, and Shahram Derakhshan, "Optimization of the Centrifugal Slurry Pump Through the Splitter Blades Position," *Proceedings of the Institution of Mechanical Engineers Part C-Journal of Mechanical Engineering Science*, vol. 236, no. 1, pp. 191-207, 2022. [CrossRef] [Google Scholar] [Publisher Link]

[6] Jiantao Zhao et al., "Energy-Saving Oriented Optimization Design of The Impeller and Volute of Multi-Stage Double-Suction Centrifugal Pump Using Artificial Neural Network," *Engineering Applications of Computational Fluid Mechanics*, vol. 16, no. 1, pp. 1974-2001, 2022. [CrossRef] [Google Scholar] [Publisher Link]

[7] Haichao Sun et al., "Parametric Analysis and Optimization Design of the Twin-Volute for a New Type of Dishwasher Pump," *Processes*, vol. 11, no. 305, pp. 1-20, 2023. [CrossRef] [Google Scholar] [Publisher Link]

[8] Yijia Cheng et al., "The Influence of Different Working Fluid Temperatures on the Hydraulic Performance of Magnetic Vortex Pumps," *Water*, vol. 16, no. 11, pp. 1-19, 2024. [CrossRef] [Google Scholar] [Publisher Link]

[9] José C. Jiménez-García et al., "Comprehensive Review of Organic Rankine Cycles," *Processes*, vol. 11, no. 1982, pp. 1-31, 2023. [CrossRef] [Google Scholar] [Publisher Link]

[10] Ashwni, and Ahmad Faizan Sherwani, "Exergy Analysis and Multi-Objective Optimization of ORC using NSGA-II," *International Journal of Exergy*, vol. 40, pp. 130-143, 2023. [CrossRef] [Google Scholar] [Publisher Link]

[11] The Process Technology and Operator Academy, Weaver Xtreme Theme Website, 2024. [Online]. Available: https://www.processtechacademy.com/

[12] Akterm Mekanik Website, Organic Rankine Cycle Systems, 2024. [Online]. Available: https://www.aktermmekanik.com.tr/en/service/organic-rankine-cycle-systems/

[13] Xiaohui Yu, Jiabao Geng, and Zhi Gao, "Thermal-Economic Analysis of An Organic Rankine Cycle System with Direct Evaporative Condenser," *Journal of Advanced Thermal Science Research*, vol. 10, pp. 41-58, 2023. [CrossRef] [Google Scholar] [Publisher Link]

[14] Weidong Cao et al., "Validation and Simulation of Cavitation Flow in A Centrifugal Pump by Filter-Based Turbulence Model," *Engineering applications of computational fluid mechanics*, vol. 16, no.1, pp. 1724-1738, 2022. [CrossRef] [Google Scholar] [Publisher Link]

[15] Levon Gevorkov, and José Luis Domínguez-García, "Experimental Hardware-in-the-Loop Centrifugal Pump Simulator for Laboratory Purposes," *Processes*, vol. 11, no. 4, pp. 1-14, 2023. [CrossRef] [Google Scholar] [Publisher Link]

[16] Hye In Kim et al., "Development of Ultra-Low Specific Speed Centrifugal Pumps Design Method for Small Liquid Rocket Engines," *Aerospace*, vol. 9, no. 9, pp. 1-19, 2022. [CrossRef] [Google Scholar] [Publisher Link]

[17] Lufeng Zhu et al., "Systematic Investigation on the Damage Characteristics of Fish in Axial Flow Pumps," *Processes*, vol. 10, no. 11, pp. 1-19, 2022. [CrossRef] [Google Scholar] [Publisher Link]

[18] Araceli Martin-Candilejo, David Santillán, and Luis Garrote, "Pump Efficiency Analysis for Proper Energy Assessment in Optimization of Water Supply Systems," *Water*, vol. 12, no. 132, pp. 1-18, 2020. [CrossRef] [Google Scholar] [Publisher Link]

[19] Peng Liu et al., "Effects of Fluid Viscosity and Two-Phase Flow on Performance of ESP," *Energies*, vol. 13, no. 20, pp. 1-20, 2020. [CrossRef] [Google Scholar] [Publisher Link]

[20] Mohamed Hassan Gobran et al., "Numerical Simulation of Centrifugal Pump and Effect of Impeller Geometry on Its Performance," *Engineering and Applied Sciences*, vol. 4, no. 2, pp. 21-29, 2019. [CrossRef] [Google Scholar] [Publisher Link]

[21] E. Q. Mohammad, S.Vladislav, and B. Pavol, "Analysis Performance Characteristics of Centrifugal Pumps," *Mm Science Journal*, pp. 1151-1159, 2016. [CrossRef] [Google Scholar] [Publisher Link]